JACS
JOURNAL OF THE AMERICAN CHEMICAL SOCIETY
pubs.acs.org/JACS
Article

Superconductivity in a Layered Cobalt Oxychalcogenide Na_2CoSe_2O with a Triangular Lattice

Jingwen Cheng,[‖] Jianli Bai,[‖] Binbin Ruan, Pinyu Liu, Yu Huang, Qingxin Dong, Yifei Huang, Yingrui Sun, Cundong Li, Libo Zhang, Qiaoyu Liu, Wenliang Zhu, Zhian Ren, and Genfu Chen*

Cite This: J. Am. Chem. Soc. 2024, 146, 5908−5915

Read Online

ACCESS | Metrics & More | Article Recommendations | Supporting Information

ABSTRACT: Unconventional superconductivity in bulk materials under ambient pressure is extremely rare among the 3d transition metal compounds outside the layered cuprates and iron-based family. It is predominantly linked to highly anisotropic electronic properties and quasi-two-dimensional (2D) Fermi surfaces. To date, the only known example of a Co-based exotic superconductor is the hydrated layered cobaltate, $Na_xCoO_2{\cdot}yH_2O$, and its superconductivity is realized in the vicinity of a spin-1/2 Mott state. However, the nature of the superconductivity in these materials is still a subject of intense debate, and therefore, finding a new class of superconductors will help unravel the mysteries of their unconventional superconductivity. Here, we report the discovery of superconductivity at ∼6.3 K in our newly synthesized layered compound Na_2CoSe_2O, in which the edge-shared $CoSe_6$ octahedra form $[CoSe_2]$ layers with a perfect triangular lattice of Co ions. It is the first 3d transition metal oxychalcogenide superconductor with distinct structural and chemical characteristics. Despite its relatively low T_C, this material exhibits very high superconducting upper critical fields, $\mu_0H_{C2}(0)$, which far exceeds the Pauli paramagnetic limit by a factor of 3−4. First-principles calculations show that Na_2CoSe_2O is a rare example of a negative charge transfer superconductor. This cobalt oxychalcogenide with a geometrical frustration among Co spins shows great potential as a highly appealing candidate for the realization of unconventional and/or high-T_C superconductivity beyond the well-established Cu- and Fe-based superconductor families and opens a new field in the physics and chemistry of low-dimensional superconductors.

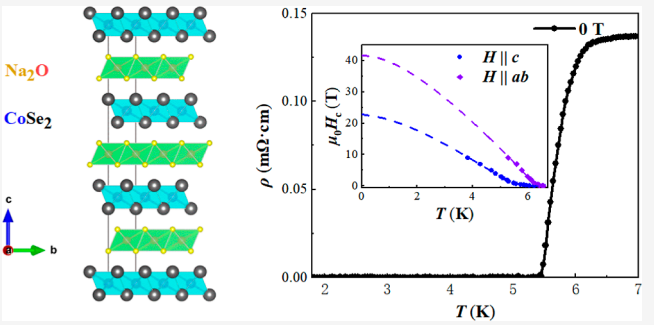

INTRODUCTION

After the discovery of superconductivity with high T_C in the iron-based family,[1] extensive work has been conducted on cobalt analogues, *Ln*Co*Pn*O (*Ln* = lanthanoids; *Pn* = P or As), $AeCo_2Pn_2$ (*Ae* = alkali earths), and ACo_2Ch_2 (*A* = alkali metal, *Ch* = S, Se, or Te) to understand their physical properties and the origin of superconductivity in iron-based superconductors since the cobalt is next to iron and has just one more electron than iron.[4−6] Although these compounds have crystal structures and Fermi surfaces similar to those of their iron-based counterparts, and their magnetism was largely tuned by size and electronic effects from changing the interlayer spacing of [Co*Pn*] or [Co*Ch*], unfortunately, no superconductivity has been reported so far in such tetragonal Co-based materials. On the other hand, there is a hydrated layered cobaltate, $Na_xCoO_2{\cdot}yH_2O$, where the cobalt ions (S = 1/2) lie on a triangular lattice, which was discovered to exhibit superconductivity at around 5 K 2 decades ago.[2] Superconductivity on such a 2D triangular lattice $[CoO_2]$ layer has attracted much attention because it may stabilize novel resonating valence bond (RVB) states,[3] which was not realized in copper oxides with the 2D square lattice. Remarkably, a chiral d + id-wave topological superconducting state was theoretically proposed for this material.[7] The vicinity of strongly correlated properties and frustrated magnetism would make this material the most exotic superconductor discovered so far.

However, the realization of high-quality samples of $Na_xCoO_2{\cdot}yH_2O$ is still a big challenge to date, in which superconductivity occurs only in the low Na content region (x = 0.22−0.47) and when water is incorporated into its structure.[8−10] The control of the Na composition and the amount of water are the two key factors limiting the realization of a single phase of $Na_xCoO_2{\cdot}yH_2O$ with good superconducting properties. Furthermore, this compound is chemically unstable at ambient temperature and humidity, which makes its handling and characterization problematic.[10] Accordingly, the nature of the superconductivity in this

Received: October 26, 2023
Revised: February 12, 2024
Accepted: February 12, 2024
Published: February 23, 2024

https://doi.org/10.1021/jacs.3c11968
J. Am. Chem. Soc. 2024, 146, 5908−5915

material is still under debate due to the lack of well-reproducible and reliable experimental results. Hence, exploring its possible analogues will deepen our understanding of the hydrated sodium cobaltate superconductor physics.

In this work, we have successfully synthesized a new cobalt oxychalcogenide, i.e., Na_2CoSe_2O, in the Na−Co−Se−O system. This compound has a layered structure composed of alternate stacking of edge-sharing Na_6O octahedra and $CoSe_6$ octahedra, in which Co atoms form a 2D triangular lattice, analogous to the hydrated sodium cobaltate, $Na_xCoO_2{\cdot}yH_2O$, while the $[CoSe_2]$ layer acts as the conducting layer instead of the $[CoO_2]$ layer, and the $[Na_2O]$ layer acts as the insulating layer instead of $[Na_x(H_2O)_y]$. Superconductivity was observed with T_C values up to 6.3 K in the compound. Like the $[CuO_2]$ plane in the cuprates and the $[Fe_2Pc_2]$ (*Pc*: anions of P, As, S, Se, or Te) layer in the iron-based family, the geometric frustrated cobalt dichalcogenide layer, $[CoSe_2]$, is believed to be crucial to supporting superconductivity in such a Co-based oxychalcogenide superconductor. First-principles calculations show that states on the Fermi level (E_F) are mainly contributed by the O 2p orbitals, while the Co 3d states dominate below −1 eV. Na_2CoSe_2O serves as a rare example of a negative charge transfer superconductor. Based on the flexibility of the structure, new Co-based superconductors with various stacking structures can be designed by changing the blocking layers. Our results demonstrate a new novel family of superconductors with unique structural and chemical characteristics and offer new perspectives for the possible further increase of the superconducting transition temperature.

EXPERIMENTAL SECTION

Crystal Growth. Single crystals of Na_2CoSe_2O were produced by a solid-state reaction of Na_2O_2 (95%, shot), NaSe, and CoSe. NaSe was synthesized in liquid ammonia from Na (2N5, lump) and Se (5N, shot) in stoichiometric quantities. CoSe was prepared from elemental Co (2N8, powder) and Se at 600 °C for 20 h. These reactants (in total 3g) were then mixed in stoichiometric ratios, pressed, put into an alumina crucible, and finally sealed in a quartz tube filled with Ar under a pressure of 0.4 atm. The quartz tube was heated to 650 °C within 20 h, held there for 20 h, and then cooled to 450 °C over 100 h. The as-grown flaky single crystals are uniformly distributed throughout the reaction products with dimensions 0.3 × 0.5 × 0.02 mm^3 and can be separated mechanically. The crystals are unstable in moist air. Except for the heat treatment, all the material preparation procedures were carried out in an Ar-filled glovebox (O_2 and H_2O < 1 ppm).

Structure and Composition Determination. Structural analyses were done on a single-crystal diffractometer of BRUKER D8 VENTURE. A specimen of Na_2CoSe_2O, with approximate dimensions of 0.050 mm × 0.270 mm × 0.340 mm, was used for the X-ray crystallographic analysis and protected under an Ar atmosphere during data collection. A total of 1094 frames were collected. The frames were integrated with the Bruker SAINT software package by using a narrow-frame algorithm. The integration of the data using a trigonal unit cell yielded a total of 869 reflections to a maximum θ angle of 26.77° (0.79 Å resolution), of which 112 were independent (average redundancy 7.759, completeness = 96.6%, R_{int} = 5.53%, and R_{sig} = 3.17%) and 110 (98.21%) were greater than $2\sigma(F^2)$. The final cell constants are based upon the refinement of the *XYZ* centroids of 1108 reflections above 20 $\sigma(I)$ with 8.507° < 2θ < 56.33°. The ratio of minimum to maximum apparent transmission was 0.456. The structure was solved and refined using the Bruker SHELXTL Software Package[11] (more details in the Supporting Information).

The chemical compositions were checked with an energy-dispersive X-ray (EDX) spectrometer equipped with a Phenom scanning electron microscope operated at 15 kV. The EDX analysis was performed on the fresh surface cleaved from as-grown crystals. The EDX analysis confirmed the existence of four elements, Na, Co, Se, and O, with Na: Co: Se close to stoichiometric proportions (more details in the Supporting Information).

Physical Property Measurements. Resistivity and Hall coefficient measurements were performed in a Quantum Design physical property measurement system. Standard four-probe and Hall bar methods were adopted to obtain the resistivity and Hall coefficient, respectively. The magnetization was measured with a Quantum Design magnetic property measurement system. All samples used for measurements were protected by N-Grease to avoid deterioration in the air.

Theoretical Methods. First-principles calculations were performed with the density functional theory (DFT), as implemented in the QUANTUM ESPRESSO package,[12] using experimental crystallographic data. To address the Co 3d electrons, the DFT + *U* method was applied with the Hubbard *U* parameter set to 4 eV for Co. The projector augmented wave pseudopotentials of PBEsol were applied.[13,14] Monkhorst−Pack grids of 17^3 and 25^3 were used in the calculations of the charge density and density of states (DOS), respectively. The CRITIC2 package was used to perform the Bader analysis.[15] No magnetic order or spin−orbit coupling effects were considered in the calculations.

RESULTS AND DISCUSSION

Na_2CoSe_2O crystallizes in the trigonal space group $R\bar{3}m$ (no. 166), as shown in Figure 1a. The lattice parameters are

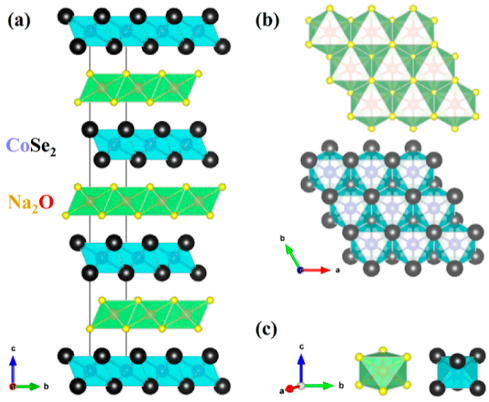

Figure 1. Crystal structure of Na_2CoSe_2O. (a) Structure of Na_2CoSe_2O, viewed from the direction of the *a*-axis. Yellow, red, blue, and black spheres represent Na, O, Co, and Se atoms, respectively. (b) Structures of the $[Na_2O]$ layer and $[CoSe_2]$ layer. (c) Structures of the single Na_6O octahedron and $CoSe_6$ octahedron.

determined to be *a* = 3.5161(9) Å, *c* = 28.745(11) Å, and *V* = 307.8(20) $Å^3$, respectively. A sufficiently large ratio, $c/a \approx 8.2$, combining the significant spatial separation between $[CoSe_2]$ layers, 9.581(67) Å, is likely to produce 2D effects in its physical properties. In fact, the weak interlayer interaction allows it to form quasi-2D flaky crystals that are easily cleaved. To the best of our knowledge, this new crystal structure is different from the existing reported ones. In general, most transition metal layered mixed-anion compounds crystallize in tetragonal space groups rather than a hexagonal space group. Although the main features of Na_2CoSe_2O, namely, $[CoSe_2]$ layers, have been described in a series of transition metal dichalcogenides (TMDs),[16] such as VSe_2, $NbSe_2$, etc., the insulating $[Na_2O]$ layers with a triangular lattice between adjacent $[CoSe_2]$ layers have never been found in any other compounds. Specifically, it is staggered by three $[Na_2O]$ layers

https://doi.org/10.1021/jacs.3c11968
J. Am. Chem. Soc. 2024, 146, 5908−5915

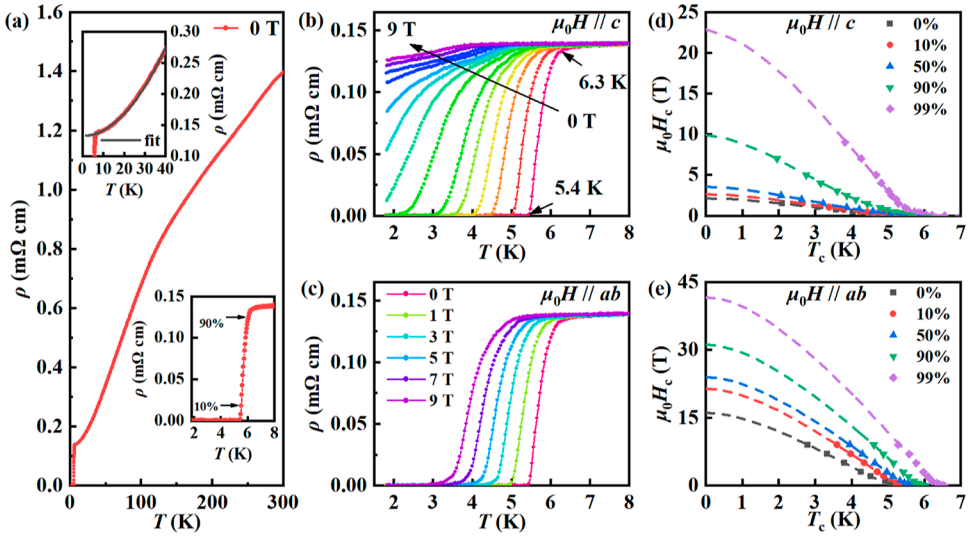

Figure 2. Superconductivity and anisotropic upper critical fields of single crystal Na_2CoSe_2O. (a) Temperature dependence of the in-plane resistivity of Na_2CoSe_2O at zero magnetic field. Upper inset: Solid line is the fitting of $\rho(T) = \rho_0 + AT^2$ with $\rho_0 = 0.132$ mΩ cm and $A = 8.8 \times 10^{-5}$ mΩ cm/K^2 for $T_C < T < 40$ K. Bottom inset: Enlarged low-temperature data, where the arrows mark the superconducting transition temperature with the 90 and 10% criteria. (b) Low-temperature dependence of the resistivity across the superconducting transition with varying magnetic fields from 0 to 9 T for $\mu_0 H \parallel c$, ($\mu_0 H$ = 0, 0.1, 0.3, 0.5, 0.75, 1, 1.5, 2, 2.5, 3, 4, 5, 7, and 9 T). (c) Low-temperature dependence of the resistivity across the superconducting transition with varying magnetic fields from 0 to 9 T for $\mu_0 H \parallel ab$. (d,e) Temperature dependence of the upper critical fields $\mu_0 H(T)$ for both directions. The dashed lines are the two-band fit (see the Supporting Information).

and three [$CoSe_2$] layers with the ABC stacking order in one unit cell, as shown in Figure 1a. [Na_2O] layers stack along (1/3, 2/3, −1/3) and [$CoSe_2$] layers stack along (2/3, 1/3, 1/3). The distance between adjacent [Na_2O] and [$CoSe_2$] layers is 4.79083 Å. Six Se (Na) atoms surround a Co (O) atom to form $CoSe_6$ (ONa_6) octahedra. For example, in the [$CoSe_2$] layer, Co atoms are located in the same plane, arranged in a triangular lattice, and Se atoms are alternately located above and below the center of the triangular lattice with the shortest Co−Co distance of 3.5161(9) Å and Co−Se bond length of 2.3994(12) Å. The nearest distance between Se atoms is also 3.5161(9) Å, and the Se−Co−Se angle is 94.23(6)° in the same Se plane, while the values are 3.266(4) Å and 85.77(6)° in different planes, respectively, forming $CoSe_6$ octahedra compressed along the *c*-axis. These edge-shared $CoSe_6$ octahedra form the [$CoSe_2$] layers, as shown in Figure 1b,c. Thus, the effect of geometric frustration caused by the triangular arrangement of magnetic atoms can be expected. In the past few decades, geometric frustration has been the subject of a number of studies because it may lead to various exotic ground states, including spin liquid, and nematic phases, especially the likely physical realization of a long-sought RVB state in triangular magnetic lattices with antiferromagnetic nearest-neighbor interactions.[17−19] In general, both the [Na_2O] and [$CoSe_2$] layers are expected to be electrically neutral, and the charge-neutral nature of the [Na_2O] and [$CoSe_2$] layers, in principle, prevents charge transfer between them; thus, the ionic state of cobalt in Na_2CoSe_2O might be Co^{4+} and its outer-shell electron is $3d^5$. And so, interesting phenomena related to geometric frustration, if the nearest-neighbor exchange interactions are antiferromagnetic, may also emerge. Indeed, as shown in the latter, magnetic susceptibility measurement does show no long-range magnetic ordering down to 6 K, at which the superconductivity sets in. Na_2CoSe_2O could thus represent a model system for studying the superconducting state in a geometrically frustrated system.

It is well-known that the hydrated sodium cobaltate, $Na_xCoO_2{\cdot}yH_2O$, is also a layered crystal structure, possessing [CoO_2] layers consisting of CoO_6 octahedra, where the [CoO_2] layers are separated by thick insulating layers of Na^+ ions and H_2O molecules. Remarkably, the atomic arrangement in essential layers, namely, the triangular lattice of Co atoms, is the same in [$CoSe_2$] layers and [CoO_2] layers, which is the most interesting and attractive structural feature that may lead to the presence of geometric magnetic frustration. As the key structural unit for superconductivity, the geometric frustrated [$CoSe_2$] layers can be simply constructed by substituting Se atoms for O atoms in [CoO_2] layers. Besides, [Na_2O] layers replacing the insulating layers of [$Na_x(H_2O)_y$] makes the layer spacing between [$CoSe_2$] layers, 9.581(67) Å, in Na_2CoSe_2O comparable to the distance of 9.8103(57) Å between [CoO_2] layers in $Na_xCoO_2{\cdot}yH_2O$. However, compared to $Na_xCoO_2{\cdot}yH_2O$, the crystals of which must be obtained by the additional chemical oxidation process from a parent compound and the Na content of which is difficult to control and identify, it is relatively easy to prepare single crystals of Na_2CoSe_2O with a well-defined structure and stoichiometry by a solid-state method only, which will be conducive to our understanding of superconducting mechanisms of the geometric frustrated systems.

Figure 2a shows the temperature dependence of the in-plane resistivity. The normal-state resistivity is on the order of 1.4 mΩ·cm at room temperature and shows an anomalous *S*-shaped temperature dependence, a character of a highly correlated electron system. As a hallmark of the Fermi liquid state formed by strong electron correlations, $\rho(T)$ also exhibits a quadratic temperature dependence over a wide low temperature range ($T_C < T < 40$ K), as shown in the upper inset of Figure 2a. The bottom inset shows the resistive superconducting transition in more detail. The onset temperature is 6.3 K, with a 10−90% transition width of ∼0.5 K, indicating the high quality of the sample. The upper critical

https://doi.org/10.1021/jacs.3c11968
J. Am. Chem. Soc. 2024, 146, 5908−5915

field H_{C2} is one of the important parameters to characterize superconductivity. To get information about H_{C2} of the Na_2CoSe_2O sample, we measured the electrical resistivity under several selected magnetic fields up to 9 T, as shown in Figure 2b,c, with the field applied parallel to the *c*-axis ($\mu_0H \parallel c$) and *ab*-plane ($\mu_0H \parallel ab$), respectively. For $\mu_0H \parallel c$, with increasing field, the transition temperature T_C shifts slowly to lower temperature and the transition width gradually becomes broader. One can see that the onset T_C moves very little (~2.5 K) at a field as high as 9 T, while the foot of the transition is shifted to substantially lower temperature. Surprisingly, in contrast to the strong broadening effect observed for $\mu_0H \parallel c$, one can find that the superconducting transition is broadened very slightly in magnetic fields up to 9 T for $\mu_0H \parallel ab$. These features are very similar to those of the high-T_C copper oxide superconductors, in which the anisotropy of the broadening phenomenon is related to the orientation of the field with respect to the Cu−O planes because of the strongly anisotropic critical fields and anisotropic pinning forces.[20,21] In our case, this is also actually understandable because the spacing distance between $[CoSe_2]$ planes is very large, making the system closer to 2D as well, as expected from its quasi-2D electronic structure (see the inset of Figure 4).

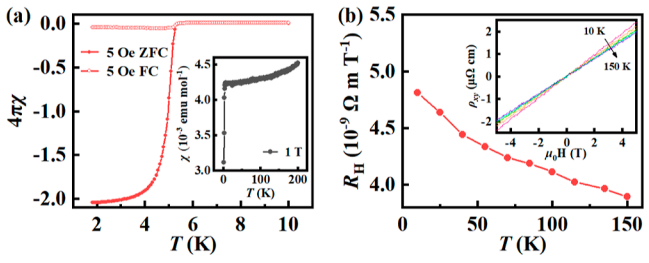

Figure 3. Magnetic susceptibility and Hall coefficient of Na_2CoSe_2O. (a) Temperature dependence of the ZFC (filled circles) and FC (open circles) magnetic susceptibility for Na_2CoSe_2O at a magnetic field of 5 Oe. The inset is the temperature dependence of the magnetic susceptibility χ (T) obtained in a magnetic field of 1 T for $\mu_0H \parallel c$. (b) Temperature dependence of the Hall coefficient R_H between 10 and 150 K. Inset: Magnetic field dependence of Hall resistivity ρ_{xy} at several temperatures for Na_2CoSe_2O.

Figure 2d,e shows $H_{C2}-T_C$ curves for both $\mu_0H \parallel c$ and $\mu_0H \parallel ab$, respectively, in which we took five values of transition temperature corresponding to the resistivity drops to 99, 90, 50, and 10% of the normal state value and zero resistivity. For each criterion of superconducting transition, $H_{C2}(T)$ lines actually display a very strong upward curvature close to T_C, which deviate from the conventional one-band Werthamer−Helfand−Hohenberg model[22] and cannot be explained by the Ginzburg−Landau theory too.[23] As for the upward curvature of $H_{C2}(T)$, several theoretical approaches have been proposed, like the mesoscopic fluctuation in disordered superconductors,[24] the Josephson tunneling between superconducting clusters,[25] the reduction of the diamagnetic pair-breaking in the stripe phase,[26] the strong spin-flip scattering,[27] the Bose−Einstein condensation of charged bosons,[28] and the mixed symmetry order parameters.[29] For example, the observed upward curvature in $Na_{0.35}CoO_2{\cdot}yH_2O$ has been considered to result from the transition between two different pairing symmetries ($s + d$) that occurs on different energy bands and gives the best fit to the experimental data.[30]

On the other hand, we noted also that a similar behavior was observed in some multiband systems such as MgB_2[31] and iron-based superconductors[32] and can be explained well within a two-band scenario with taking into account the inter- and intraband scattering.[33] In our case, the best fitted $H_{C2}(T)$ curves are shown in Figure 2d,e and can be seen to agree very well with the experimental data [more details in the Supporting Information], which seems to suggest the multiband nature of the superconductivity. Within this theoretical framework and taking the 99% criterion, the $\mu_0H_{C2}(0)$ along the *c*-axis and the *ab*-plane were calculated to be ~23 and 41 T, respectively. Both the estimated upper critical fields at zero temperature far exceed the Pauli pair-breaking limit (given by $\mu_0H_P = 1.84\ T_C \approx 11.6$ T for $T_C = 6.3$ K) in a BCS weak-coupling case.[34,35] When employing the 90% criterion, the $\mu_0H^c_{C2}(0)$ and $\mu_0H^{ab}_{C2}(0)$ were estimated to be ~9 and 31 T, respectively, and the corresponding anisotropic ratio $\gamma = \frac{H^c_{C2}(0)}{H^{ab}_{C2}(0)}$ in Na_2CoSe_2O is ~3.3, which is a little higher than that of $Sr_{1-x}K_xFe_2As_2$ with $\gamma = 2$,[36] while it is much lower than that of high T_C cuprates, for example $\gamma = 7-10$ for YBCO.[37] The high in-plane $\mu_0H_{C2}(0)$, exceeding the Pauli limiting field by a factor of 3−4, suggests a more exotic pairing mechanism in Na_2CoSe_2O. It is interesting that the upper critical field is far beyond that of $Na_{0.35}CoO_2{\cdot}1.3H_2O$ [$\mu_0H_{C2}(0) \sim 8$ T for $\mu_0H \parallel ab$].[38] Nevertheless, a topologically nontrivial superconducting pairing via the nearest neighbor antiferromagnetic superexchange in such a triangular lattice has been proposed for $Na_xCoO_2{\cdot}yH_2O$,[7] and a similar mechanism may also be involved in Na_2CoSe_2O due to the same geometric frustration, which warrants further investigation.

In order to check whether the observed SC is of a bulk nature, we performed dc magnetic susceptibility $\chi(T)$ measurements in both zero-field cooling (ZFC) and field cooling (FC) modes under a magnetic field of 5 Oe, which reveals a superconducting transition close to 5.4 K, as shown in Figure 3a, roughly corresponding to the zero-resistivity temperature in Figure 2b. The difference between ZFC and FC strongly suggests a type II superconducting nature. The superconducting volume fraction estimated from the ZFC magnetization at 2 K was much larger than 100%, without considering the demagnetization factor due to the irregular shape of the samples, which unambiguously proves the bulk superconductivity of the Na_2CoSe_2O sample. The inset of Figure 2a shows the normal-state magnetic susceptibility as a function of the temperature, $\chi(T)$, for the Na_2CoSe_2O crystals with a magnetic field of 1 T applied along the *c*-axis. Because the crystal is too small, several pieces are used, which might cause some uncertainty in the analysis of the magnetization. A drop in susceptibility at about 5 K corresponds to the superconducting transition. It should be noted that $\chi(T)$ increases monotonically with increasing temperature above T_C, seeming to indicate the existence of AF spin fluctuation in the normal state. A similar χ-T curve was also observed in $Na_{0.35}CoO_2{\cdot}1.3H_2O$, in which a significant increase with decreasing T at low temperatures was considered to be extrinsic.[39] At the present stage, the nature of magnetic interactions in Na_2CoSe_2O is not clear yet and will be the subject of further experimental investigations, which may play a crucial role in the formation of superconducting states in such a system, as discussed above.

To obtain more information about the conducting carriers, we measured the Hall coefficient in the normal state. From the

https://doi.org/10.1021/jacs.3c11968
J. Am. Chem. Soc. 2024, 146, 5908−5915

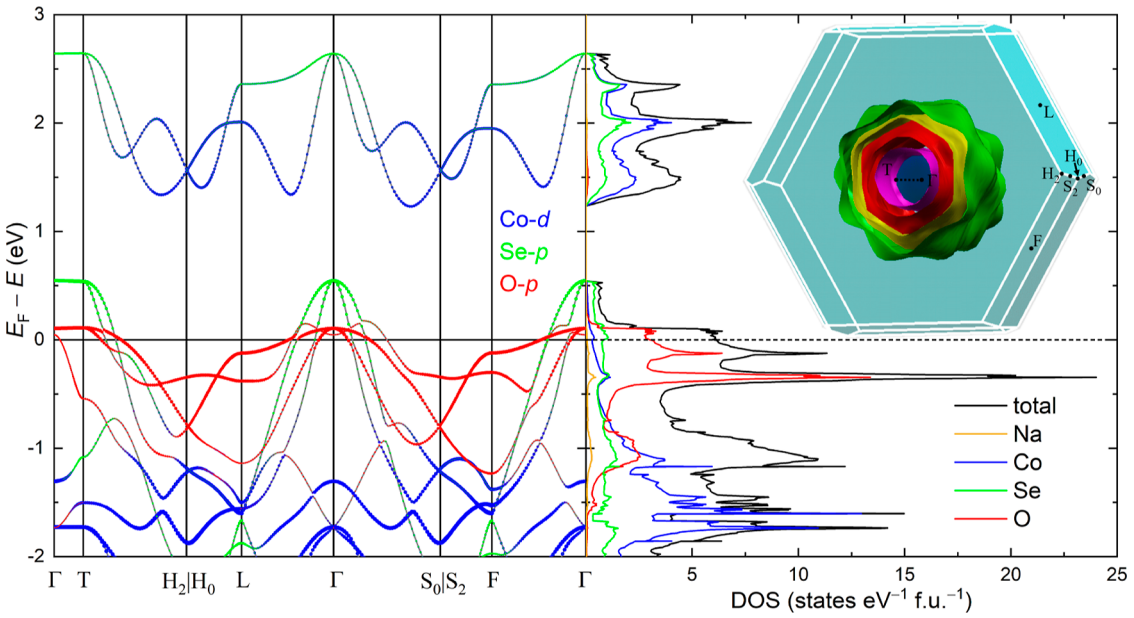

Figure 4. Band structure and Fermi surfaces of Na_2CoSe_2O by DFT + U calculations. Electronic band structure (left) and DOS (right) of Na_2CoSe_2O. Different colors represent contributions from different atoms/orbitals. The inset shows the Fermi surfaces of Na_2CoSe_2O in the first Brillouin zone, in which the high symmetry points are labeled.

$\rho_{xy}(H)$ data (inset of Figure 3b), the Hall coefficient R_H is determined through $R_H = \rho_{xy}/\mu_0 H$ and is plotted in Figure 3b, which shows a strong temperature-dependent behavior. For a metallic material, the T-dependent R_H is often explained by the multiband effect.[40] Indeed, according to the DFT calculations for Na_2CoSe_2O, five bands cross the Fermi level E_F, forming five hole pockets. Therefore, it is possible that the T-dependent R_H comes from the multiband effect. Alternatively, the T dependence of R_H could also be caused by a magnetic skew scattering mechanism,[41] which has been observed in various materials with the presence of magnetic moments. As the compound Na_2CoSe_2O contains a Co element and the Co valence state may be mainly Co IV, the skew scattering mechanism might also work here. So, here, the strong T-dependent R_H tells us that either the multiband effect or the skew scattering might be involved in the transport process in this material. Actually, a large T dependence of R_H was also observed in the iron-based and copper oxide superconductors and was regarded as one of the exotic properties.[42,43] The positive R_H over the whole temperature range measured up to 150 K suggests that holes are the dominant carriers in transport, consistent with the results of our band calculations. A rough estimation based on the relation $R_H = 1/ne$ indicates that the carrier density is rather low, for example, at 10 K, the carrier density is about 1.3×10^{21} cm^{-3}, which is similar to those of the iron-based superconductors and high-T_C cuprates.[42,43] Thus, Na_2CoSe_2O belongs to a class of poor conductors in the normal state.

Figure 4 shows the results of the DFT + U calculations. An indirect energy gap of about 0.8 eV can be identified. The E_F is located near the top of the valence bands, implying Na_2CoSe_2O to be a p-type semiconductor. There are multiple bands crossing E_F, which is consistent with the Hall/H_{C2} results. Interestingly, states on E_F are mainly contributed by the O 2p and Se 4p orbitals, while the Co 3d states dominate below −1 eV. Na_2CoSe_2O is thus a negative charge transfer material, which is as expected from the nominal oxidation state (Co^{4+}) of Co. With Co in such a high oxidation state, electrons tend to transfer from the ligand (Se) to Co, leaving additional holes in the ligand orbitals. Similar phenomena have been observed in materials with highly oxidized transition metals, such as $NaCuO_2$,[44] $NdNiO_3$,[45] and $CaFeO_3$.[46] We also note that while most of the negative charge transfer materials are insulators, Na_2CoSe_2O serves as a rare example of a negative charge transfer superconductor. The Bader analysis gives a valence configuration of $[Na_2O]^{0.43+}[CoSe_2]^{0.43-}$. In other words, electrons from the $[Na_2O]$ layers are transferred into the $[CoSe_2]$ layers, lowering the valence of Co. The Co valence in Na_2CoSe_2O is then estimated to be 3.57, which is comparable to the value of 3.46 for the superconducting $Na_{0.36}CoO_2 \cdot 1.3H_2O$.[47] The DFT calculation suggests nearly full Co $(t_{2g})^6$ orbitals, while the e_g orbitals are empty. In other words, a low-spin $(t_{2g})^6(e_g)^0$ configuration is favored. We note that although the DFT + U calculation suggests a low-spin $(t_{2g})^6$ configuration for Co, the actual spin configuration could still be $(t_{2g})^4(e_g)^2$, given that Se^{2-} is a relatively weak ligand. Note that these calculations are nonmagnetic. A future neutron diffraction study will help us determine the actual spin configuration of Co. Moreover, when the Hubbard U term is ignored, a much higher DOS for Co can be expected (see Figure S2). In both cases (with and without U), there are considerable amounts of holes on the O and Se orbitals, resulting from the aforementioned charge transfer mechanism. This means that both the $[Na_2O]$ and $[CoSe_2]$ layers may be conducting. However, the hole mobilities in these two layers can be very different. Note that the O bands are nearly flat near the Fermi level (Figure 4), while the Se bands are steeper. This means that the holes in the $[Na_2O]$ layers are heavier. The concentration of holes on ligands Se and O is as expected for negative charge transfer (NCT) compounds, and similar scenarios have been proposed in other NCT compounds such as $NdNiO_3$[45] and pressurized cuprates.[48] The Fermi surfaces of Na_2CoSe_2O consist of five sheets (see the inset of Figure 4). All of them are hole-like surfaces surrounding the Γ

https://doi.org/10.1021/jacs.3c11968
J. Am. Chem. Soc. 2024, 146, 5908−5915

point. Most of the Fermi surfaces, except for the innermost one, are quasi-2D, showing little energy dispersion along the $\Gamma-T$ path. This feature is consistent with the quasi-2D nature of the crystal structure.

Clearly, Na_2CoSe_2O shares many aspects with the cuprates and Fe-based superconductors, such as two-dimensionality, low carrier concentration, multiple bands, very high upper critical fields, and also some hints of the strong electronic correlations and AF spin fluctuation, all of which point toward an exotic superconductivity in Na_2CoSe_2O. One difference is that unlike the cuprates or iron-based superconductors, where the parent materials are AF Mott insulators or AF semimetals, Na_2CoSe_2O shows superconductivity without explicit doping, where the charge transfer acts as a self-doping effect, which, coupled with the geometrical frustration, prevents the formation of long-range magnetic ordering and eventually leads to superconductivity. It has been well-established that the 2D $[CuO_2]$ or $[Fe_2Pc_2]$ conducting layers modulated by the blocking layers (serve as a charge reservoir) are critical for the high-T_C superconductivity, in which various types of blocking layers have been realized and several of them achieved high T_C. Similarly, since the $[CoSe_2]$ layer is the key structural unit in such a Co-based superconductor, analogous superconductors could be designed by modifying the blocking layers of $[Na_2O]$. Finding new components for the blocking layers is the key to discovering new superconductors with a higher T_C. Additionally, building up multilayered cobalt chalcogenides may also lead to higher T_C, as in the case of cuprates.[49] Multilayered iron-based superconductors with square lattices are still not discovered, but multilayered systems with triangular lattices have been achieved in iron sulfide (Smythite, Fe_3S_4) and chromium selenide $Na_{0.7}Cr_{2.3}Se_4$.[50,51] Certainly, there are many other candidates with 3d transition-metal-based 2D triangular lattices, which have chalcogenide chemistry similar to that of cobalt. This layered structure provides new hope and opportunity for exploring the exotic superconductivity in TMDs.

Finally, we would like to point out that much of the attention has been focused in recent years on the 3d transition metal oxychalcogenides with square lattices, in which the possibility of high-T_C superconductivity was theoretically predicted upon doping the Mott insulating state with electrons or holes.[52,53] Nevertheless, superconductivity has not yet been observed in such oxychalcogenides by now. Our result demonstrates for the first time, to our knowledge, that the Co-based oxychalcogenide is indeed superconducting but with a triangular lattice. Compared to the square lattice in iron-based superconductors, a triangular lattice may lead to an unconventional ground state and/or form geometric frustration in magnetic systems, which has aroused great interest in the field of strongly correlated electron systems. For example, in addition to the superconductivity in $Na_xCoO_2{\cdot}yH_2O$, the discovery of the heavy Fermion behavior in the pyrochlore compound LiV_2O_4,[54,55] as well as the newly discovered Kagome lattice superconductors AV_3Sb_5 (A = K, Rb, and Cs),[56,57] has stimulated intensive studies of frustrated electron systems. There is no doubt that the triangular lattice in Na_2CoSe_2O offers an exciting playground and challenges for superconductivity, and there is still high potential to study and discover a novel type of superconductor in such a triangular system.

CONCLUSIONS

In conclusion, we have discovered a new layered oxychalcogenide superconductor. Its crystal structure, built by alternate stacking of $[CoSe_2]$ conducting layers and $[Na_2O]$ blocking layers, is similar to those of layered cuprates and the Fe-based family. One difference is that, instead of the well-defined square lattices in Cu−O and Fe−As plane, Co atoms form a two-dimensional triangular lattice in Na_2CoSe_2O, in which the superconducting state originates from the geometric frustrated $[CoSe_2]$ layers. The preliminary physical property measurements indicate that this system also has many unique features, such as low carrier concentration, multiple bands, and high upper critical fields, all of which point toward an exotic superconductivity in Na_2CoSe_2O. Based on the flexibility of the structure, new Co-based superconductors with various stacking structures can be designed by changing the blocking layers.

Our studies expand the categories of unconventional superconductors in 3d transition metal compounds and open a door for finding new potential high-T_C superconductors. It would be of interest in future studies to explore the similarities and differences between the layered cobalt oxychalcogenide and hydrated cobaltate from both theoretical and experimental perspectives, as well as to infer something universal about unconventional superconductivity between these 2D geometrically frustrated lattices and the well-defined square lattices of cuprates and the iron-based family, which will help resolve their elusive superconducting mechanism.

ASSOCIATED CONTENT

Supporting Information

The Supporting Information is available free of charge at https://pubs.acs.org/doi/10.1021/jacs.3c11968.

Detailed crystal structure analysis of Na_2CoSe_2O, EDX measurements, thermodynamic stability and HSAB rule analysis of Na_2CoSe_2O, two-band model analysis of $H_{C2}(T)$ in two directions, and DFT results without U (PDF)

Accession Codes

CCDC 2303881 contains the supplementary crystallographic data for this paper. These data can be obtained free of charge via www.ccdc.cam.ac.uk/data_request/cif, or by emailing data_request@ccdc.cam.ac.uk, or by contacting The Cambridge Crystallographic Data Centre, 12 Union Road, Cambridge CB2 1EZ, UK; fax: +44 1223 336033.

AUTHOR INFORMATION

Corresponding Author

Genfu Chen − *Institute of Physics and Beijing National Laboratory for Condensed Matter Physics, Chinese Academy of Sciences, Beijing 100190, China; School of Physical Sciences, University of Chinese Academy of Sciences, Beijing 100049, China; Songshan Lake Materials Laboratory, Dongguan, Guangdong 523808, China*; Email: gfchen@iphy.ac.cn

Authors

Jingwen Cheng − *Institute of Physics and Beijing National Laboratory for Condensed Matter Physics, Chinese Academy of Sciences, Beijing 100190, China; School of Physical Sciences, University of Chinese Academy of Sciences, Beijing 100049, China*; orcid.org/0000-0001-5587-8951

Jianli Bai − *Institute of Physics and Beijing National Laboratory for Condensed Matter Physics, Chinese Academy of Sciences, Beijing 100190, China; School of Physical Sciences, University of Chinese Academy of Sciences, Beijing 100049, China*

Binbin Ruan − *Institute of Physics and Beijing National Laboratory for Condensed Matter Physics, Chinese Academy of Sciences, Beijing 100190, China;* orcid.org/0000-0003-4642-7782

Pinyu Liu − *Institute of Physics and Beijing National Laboratory for Condensed Matter Physics, Chinese Academy of Sciences, Beijing 100190, China; School of Physical Sciences, University of Chinese Academy of Sciences, Beijing 100049, China*

Yu Huang − *Institute of Physics and Beijing National Laboratory for Condensed Matter Physics, Chinese Academy of Sciences, Beijing 100190, China; School of Physical Sciences, University of Chinese Academy of Sciences, Beijing 100049, China*

Qingxin Dong − *Institute of Physics and Beijing National Laboratory for Condensed Matter Physics, Chinese Academy of Sciences, Beijing 100190, China*

Yifei Huang − *Institute of Physics and Beijing National Laboratory for Condensed Matter Physics, Chinese Academy of Sciences, Beijing 100190, China*

Yingrui Sun − *Institute of Physics and Beijing National Laboratory for Condensed Matter Physics, Chinese Academy of Sciences, Beijing 100190, China; School of Physical Sciences, University of Chinese Academy of Sciences, Beijing 100049, China*

Cundong Li − *Institute of Physics and Beijing National Laboratory for Condensed Matter Physics, Chinese Academy of Sciences, Beijing 100190, China; School of Physical Sciences, University of Chinese Academy of Sciences, Beijing 100049, China*

Libo Zhang − *Institute of Physics and Beijing National Laboratory for Condensed Matter Physics, Chinese Academy of Sciences, Beijing 100190, China; School of Physical Sciences, University of Chinese Academy of Sciences, Beijing 100049, China*

Qiaoyu Liu − *Institute of Physics and Beijing National Laboratory for Condensed Matter Physics, Chinese Academy of Sciences, Beijing 100190, China; School of Physical Sciences, University of Chinese Academy of Sciences, Beijing 100049, China*

Wenliang Zhu − *Institute of Physics and Beijing National Laboratory for Condensed Matter Physics, Chinese Academy of Sciences, Beijing 100190, China*

Zhian Ren − *Institute of Physics and Beijing National Laboratory for Condensed Matter Physics, Chinese Academy of Sciences, Beijing 100190, China; School of Physical Sciences, University of Chinese Academy of Sciences, Beijing 100049, China;* orcid.org/0000-0003-4308-7372

Complete contact information is available at: https://pubs.acs.org/10.1021/jacs.3c11968

Author Contributions

[‖]J.C. and J.B. contributed equally to this work.

Notes

The authors declare no competing financial interest.

■ ACKNOWLEDGMENTS

This work was supported by the Ministry of Science and Technology of China (grant no. 2022YFA1403903), the National Natural Science Foundation of China (grant no. 12274440), the Strategic Priority Research Program (B) of Chinese Academy of Sciences (grant no. XDB33010100), and the Synergetic Extreme Condition User Facility (SECUF).

■ REFERENCES

(1) Kamihara, Y.; Watanabe, T.; Hirano, M.; Hosono, H. Iron-Based Layered Superconductor La[$O_{1-x}F_x$]FeAs (x = 0.05−0.12) with T_c = 26 K. *J. Am. Chem. Soc.* **2008**, *130* (11), 3296−3297.

(2) Takada, K.; Sakurai, H.; Takayama-Muromachi, E.; Izumi, F.; Dilanian, R. A.; Sasaki, T. Superconductivity in two-dimensional CoO_2 layers. *Nature* **2003**, *422* (6927), 53−55.

(3) Baskaran, G. Electronic Model for CoO_2 layer based systems: chiral resonating valence bond metal and superconductivity. *Phys. Rev. Lett.* **2003**, *91* (9), 097003.

(4) Ohta, H.; Yoshimura, K. Anomalous magnetization in the layered itinerant ferromagnet LaCoAsO. *Phys. Rev. B* **2009**, *79* (18), 184407.

(5) Sefat, A. S.; Singh, D. J.; Jin, R.; McGuire, M. A.; Sales, B. C.; Mandrus, D. Renormalized behavior and proximity of $BaCo_2As_2$ to a magnetic quantum critical point. *Phys. Rev. B* **2009**, *79* (2), 024512.

(6) Yang, J.; Chen, B.; Wang, H.; Mao, Q.; Imai, M.; Yoshimura, K.; Fang, M. Magnetic properties in layered ACo_2Se_2(*A* = K, Rb, Cs) with the $ThCr_2Si_2$-type structure. *Phys. Rev. B* **2013**, *88* (6), 064406.

(7) Zhou, S.; Wang, Z. Nodal *d* + *id* pairing and topological phases on the triangular lattice of $Na_xCoO_2{\cdot}yH_2O$: evidence for an unconventional superconducting state. *Phys. Rev. Lett.* **2008**, *100* (21), 217002.

(8) Chen, D. P.; Chen, H. C.; Maljuk, A.; Kulakov, A.; Zhang, H.; Lemmens, P.; Lin, C. T. Single-crystal growth and investigation of Na_xCoO_2 and $Na_xCoO_2{\cdot}yH_2O$. *Phys. Rev. B* **2004**, *70* (2), 024506.

(9) Ueland, B. G.; Schiffer, P.; Schaak, R. E.; Foo, M. L.; Miller, V. L.; Cava, R. J. Specific heat study of the $Na_{0.3}CoO_2{\cdot}1.3H_2O$ superconductor: influence of the complex chemistry. *Phys. C* **2004**, *402* (1−2), 27−30.

(10) Schaak, R. E.; Klimczuk, T.; Foo, M. L.; Cava, R. J. Superconductivity phase diagram of $Na_xCoO_2{\cdot}1.3H_2O$. *Nature* **2003**, *424* (6948), 527−529.

(11) Sheldrick, G. M. A short history of *SHELX*. *Acta Crystallogr., Sect. A: Found. Crystallogr.* **2008**, *64* (1), 112−122.

(12) Giannozzi, P.; Baroni, S.; Bonini, N.; Calandra, M.; Car, R.; Cavazzoni, C.; Ceresoli, D.; Chiarotti, G. L.; Cococcioni, M.; Dabo, I.; et al. QUANTUM ESPRESSO: a modular and open-source software project for quantum simulations of materials. *J. Phys.: Condens. Matter* **2009**, *21* (39), 395502.

(13) Dal Corso, A. Pseudopotentials periodic table: From H to Pu. *Comput. Mater. Sci.* **2014**, *95*, 337−350.

(14) Perdew, J. P.; Ruzsinszky, A.; Csonka, G. I.; Vydrov, O. A.; Scuseria, G. E.; Constantin, L. A.; Zhou, X.; Burke, K. Restoring the Density-Gradient Expansion for Exchange in Solids and Surfaces. *Phys. Rev. Lett.* **2008**, *100* (13), 136406.

(15) Otero-de-la-Roza, A.; Johnson, E. R.; Luaña, V. Critic2: A program for real-space analysis of quantum chemical interactions in solids. *Comput. Phys. Commun.* **2014**, *185* (3), 1007−1018.

(16) Wilson, J. A.; Yoffe, A. D. The transition metal dichalcogenides discussion and interpretation of the observed optical, electrical and structural properties. *Adv. Phys.* **1969**, *18* (73), 193−335.

(17) Moessner, R.; Sondhi, S. L. Resonating Valence Bond Phase in the Triangular Lattice Quantum Dimer Model. *Phys. Rev. Lett.* **2001**, *86* (9), 1881−1884.

(18) Anderson, P. W. Resonating valence bonds: A new kind of insulator? *Mater. Res. Bull.* **1973**, *8* (2), 153−160.

(19) Tsunetsugu, H.; Arikawa, M. Spin Nematic Phase in *S* = 1 Triangular Antiferromagnets. *J. Phys. Soc. Jpn.* **2006**, *75* (8), 083701.

(20) Palstra, T. T. M.; Batlogg, B.; Schneemeyer, L. F.; Waszczak, J. V. Thermally activated dissipation in $Bi_{2.2}Sr_2Ca_{0.8}Cu_2O_{8+\delta}$. *Phys. Rev. Lett.* **1988**, *61* (14), 1662−1665.
(21) Welp, U.; Kwok, W. K.; Crabtree, G. W.; Vandervoort, K. G.; Liu, J. Z. Magnetic measurements of the upper critical field of $YBa_2Cu_3O_{7-\delta}$ single crystals. *Phys. Rev. Lett.* **1989**, *62* (16), 1908−1911.
(22) Werthamer, N. R.; Helfand, E.; Hohenberg, P. C. Temperature and purity dependence of the superconducting critical field, H_{C2}. III. Electron spin and spin-orbit effects. *Phys. Rev.* **1966**, *147* (1), 295−302.
(23) Ginzburg, V. L.; Landau, L. D. On the Theory of Superconductivity. *Zh. Eksp. Teor. Fiz.* **1950**, *20*, 1064−1082.
(24) Spivak, B.; Zhou, F. Mesoscopic effects in disordered superconductors near H_{C2}. *Phys. Rev. Lett.* **1995**, *74* (14), 2800−2803.
(25) Geshkenbein, V. B.; Ioffe, L. B.; Millis, A. J. Theory of the resistive transition in overdoped $Tl_2Ba_2CuO_{6+\delta}$: Implications for the vortex viscosity and the quasiparticle scattering rate in high-T_C superconductors. *Phys. Rev. Lett.* **1998**, *80* (26), 5778−5781.
(26) Mierzejewski, M.; Maśka, M. M. Upper critical field for underdoped high-T_C superconductors: Pseudogap and stripe phase. *Phys. Rev. B* **2002**, *66* (21), 214527.
(27) Ovchinnikov, Y. N.; Kresin, V. Z. Critical magnetic field in layered superconductors. *Phys. Rev. B* **1995**, *52* (5), 3075−3078.
(28) Alexandrov, A. S.; Zavaritsky, V. N.; Liang, W. Y.; Nevsky, P. L. Resistive upper critical field of high-T_C single crystals of $Bi_2Sr_2CaCu_2O_8$. *Phys. Rev. Lett.* **1996**, *76* (6), 983−986.
(29) Joynt, R. Upward curvature of H_{C2} in high-T_C superconductors: Possible evidence for *s-d* pairing. *Phys. Rev. B* **1990**, *41* (7), 4271−4277.
(30) Maśka, M. M.; Mierzejewski, M.; Andrzejewski, B.; Foo, M. L.; Cava, R. J.; Klimczuk, T. Possible singlet-to-triplet pairing transition in $Na_xCoO_2{\bullet}yH_2O$. *Phys. Rev. B* **2004**, *70* (14), 144516.
(31) De Lima, O.; Ribeiro, R.; Avila, M.; Cardoso, C.; Coelho, A. Anisotropic Superconducting Properties of Aligned MgB_2 Crystallites. *Phys. Rev. Lett.* **2001**, *86* (26), 5974−5977.
(32) Hunte, F.; Jaroszynski, J.; Gurevich, A.; Larbalestier, D. C.; Jin, R.; Sefat, A. S.; McGuire, M. A.; Sales, B. C.; Christen, D. K.; Mandrus, D. Two-band superconductivity in $LaFeAsO_{0.89}F_{0.11}$ at very high magnetic fields. *Nature* **2008**, *453* (7197), 903−905.
(33) Gurevich, A. Enhancement of the upper critical field by nonmagnetic impurities in dirty two-gap superconductors. *Phys. Rev. B* **2003**, *67* (18), 184515.
(34) Chandrasekhar, B. A note on the maximum critical field of high field superconductors. *Appl. Phys. Lett.* **1962**, *1* (1), 7−8.
(35) Clogston, A. M. Upper Limit for the Critical Field in Hard Superconductors. *Phys. Rev. Lett.* **1962**, *9* (6), 266−267.
(36) Chen, G. F.; Li, Z.; Dong, J.; Li, G.; Hu, W. Z.; Zhang, X. D.; Song, X. H.; Zheng, P.; Wang, N. L.; Luo, J. L. Transport and anisotropy in single-crystalline $SrFe_2As_2$ and $A_{0.6}K_{0.4}Fe_2As_2$ (A = Sr, Ba) superconductors. *Phys. Rev. B* **2008**, *78* (22), 224512.
(37) Nanda, K. K. Temperature dependence of upper critical field and anisotropy of $YBa_2Cu_3O_7$. *Phys. C* **1996**, *265* (1−2), 26−30.
(38) Sasaki, T.; Badica, P.; Yoneyama, N.; Yamada, K.; Togano, K.; Kobayashi, N. Superconducting Properties under Magnetic Field in $Na_{0.35}CoO_2{\cdot}1.3H_2O$ Single Crystal. *J. Phys. Soc. Jpn.* **2004**, *73* (5), 1131−1134.
(39) Jin, R.; Sales, B. C.; Khalifah, P.; Mandrus, D. Observation of Bulk Superconductivity in $Na_xCoO_2{\cdot}yH_2O$ and $Na_xCoO_2{\cdot}yD_2O$ powder and single crystals. *Phys. Rev. Lett.* **2003**, *91* (21), 217001.
(40) Beer, A. C. The Hall effect and related phenomena. *Solid-State Electron.* **1966**, *9* (5), 339−351.
(41) Nagaosa, N.; Sinova, J.; Onoda, S.; Macdonald, A. H.; Ong, N. P. Anomalous Hall effect. *Rev. Mod. Phys.* **2010**, *82* (2), 1539−1592.
(42) Chen, G. F.; Li, Z.; Li, G.; Zhou, J.; Wu, D.; Dong, J.; Hu, W. Z.; Zheng, P.; Chen, Z. J.; Yuan, H. Q.; et al. Superconducting Properties of the Fe-Based Layered Superconductor $LaFeAsO_{0.9}F_{0.1-\delta}$. *Phys. Rev. Lett.* **2008**, *101* (5), 057007.
(43) Harris, J. M.; Yan, Y. F.; Ong, N. P. Experimental test of the T^2 law for the Hall angle from T_C to 500 K in oxygen-reduced $YBa_2Cu_3O_{6+x}$ crystals. *Phys. Rev. B* **1992**, *46* (21), 14293−14296.
(44) Mizokawa, T.; Namatame, H.; Fujimori, A.; Akeyama, K.; Kondoh, H.; Kuroda, H.; Kosugi, N. Origin of the band gap in the negative charge-transfer-energy compound $NaCuO_2$. *Phys. Rev. Lett.* **1991**, *67* (12), 1638−1641.
(45) Bisogni, V.; Catalano, S.; Green, R. J.; Gibert, M.; Scherwitzl, R.; Huang, Y.; Strocov, V. N.; Zubko, P.; Balandeh, S.; Triscone, J. M.; et al. Ground-state oxygen holes and the metal-insulator transition in the negative charge-transfer rare-earth nickelates. *Nat. Commun.* **2016**, *7* (1), 13017.
(46) Rogge, P. C.; Chandrasena, R. U.; Cammarata, A.; Green, R. J.; Shafer, P.; Lefler, B. M.; Huon, A.; Arab, A.; Arenholz, E.; Lee, H. N.; et al. Electronic structure of negative charge transfer $CaFeO_3$ across the metal-insulator transition. *Phys. Rev. Mater.* **2018**, *2* (1), 015002.
(47) Karppinen, M.; Asako, I.; Motohashi, T.; Yamauchi, H. Oxidation State of Cobalt in the $Na_xCoO_{2-\delta}{\cdot}yH_2O$ Superconductor. *Chem. Mater.* **2004**, *16* (9), 1693−1696.
(48) Song, J.-P.; Clay, R. T.; Mazumdar, S. Valence transition theory of the pressure-induced dimensionality crossover in superconducting $Sr_{14-x}Ca_xCu_{24}O_{41}$. *Phys. Rev. B* **2023**, *108* (13), 134510.
(49) Schilling, A.; Jeandupeux, O.; Guo, J. D.; Ott, H. R. Magnetization and resistivity study on the 130 K superconductor in the Hg-Ba-Ca-Cu-O system. *Phys. C* **1993**, *216* (1−2), 6−11.
(50) Erd, R. C.; Evans, H. T. Jr.; Richter, D. H. Smythite, A New Iron Sulfide, and Associated Pyrrhotite from Indiana. *Am. Mineral.* **1957**, *42* (5−6), 309−333.
(51) Tigchelaar, D.; Haange, R. J.; Wiegers, G. A.; van Bruggen, C. F. The synthesis, structure and physical properties of a non-stoichiometric sodium chromium selenide, $Na_{0.34}Cr_{1.15}Se_2$. *Mater. Res. Bull.* **1981**, *16* (6), 729−739.
(52) Zhu, J.-X.; Yu, R.; Wang, H.; Zhao, L. L.; Jones, M. D.; Dai, J.; Abrahams, E.; Morosan, E.; Fang, M.; Si, Q. Band Narrowing and Mott Localization in Iron Oxychalcogenides $La_2O_2Fe_2O(Se,S)_2$. *Phys. Rev. Lett.* **2010**, *104* (21), 216405.
(53) Le, C.; Qin, S.; Hu, J. Electronic physics and possible superconductivity in layered orthorhombic cobalt oxychalcogenides. *Sci. Bull.* **2017**, *62* (8), 563−571.
(54) Lohmann, M.; Hemberger, J.; Nicklas, M.; Krug von Nidda, H. A.; Loidl, A.; Klemm, M.; Obermeier, G.; Horn, S. LiV_2O_4: a heavy-fermion transition metal oxide? *Phys. B* **1999**, *259*−*261*, 963−964.
(55) Urano, C.; Nohara, M.; Kondo, S.; Sakai, F.; Takagi, H.; Shiraki, T.; Okubo, T. LiV_2O_4 Spinel as a Heavy-Mass Fermi Liquid: Anomalous Transport and Role of Geometrical Frustration. *Phys. Rev. Lett.* **2000**, *85* (5), 1052−1055.
(56) Ortiz, B. R.; Gomes, L. C.; Morey, J. R.; Winiarski, M.; Bordelon, M.; Mangum, J. S.; Oswald, I. W. H.; Rodriguez-Rivera, J. A.; Neilson, J. R.; Wilson, S. D.; et al. New kagome prototype materials: discovery of KV_3Sb_5, RbV_3Sb_5, and CsV_3Sb_5. *Phys. Rev. Mater.* **2019**, *3* (9), 094407.
(57) Ortiz, B. R.; Teicher, S. M.; Hu, Y.; Zuo, J. L.; Sarte, P. M.; Schueller, E. C.; Abeykoon, A. M.; Krogstad, M. J.; Rosenkranz, S.; Osborn, R.; et al. CsV_3Sb_5: A Z_2 Topological Kagome Metal with a Superconducting Ground State. *Phys. Rev. Lett.* **2020**, *125* (24), 247002.

https://doi.org/10.1021/jacs.3c11968
J. Am. Chem. Soc. 2024, 146, 5908−5915